Cooling of cesium atoms by collective emission inside an optical resonator

Adam T. Black, Hilton W. Chan, and Vladan Vuletić
Department of Physics, Stanford University, Stanford, California 94305-4060

Abstract

We observe collective emission when a sample of cold cesium atoms inside a vertically oriented optical cavity is illuminated by a horizontal standing wave. The enhanced cavity emission is accompanied by strong velocity-dependent forces on the atoms, that lead to slowing and cooling of a falling sample. The resonator-induced forces are substantially larger than predicted for single two-level atoms, resulting in temperatures well below the atomic and cavity Doppler limits.

1 Introduction

Doppler cooling [1], and its counterpart for trapped particles, sideband cooling [2], have provided the basis for some of the most fascinating developments in atomic physics. The experiments made possible by laser cooling range from precision spectroscopy and manipulation of single particles [3] to collective quantum phenomena such as the Bose-Einstein condensation of dilute atomic gases [4]. The notable exception is hydrogen, where condensation has been achieved by a combination of cryogenic and evaporative techniques [5].

Both Doppler and sideband cooling require a small red detuning on the order of the motional effect (Doppler shift in the case of free particles, trap vibration frequency in the case of trapped ions) between the incident light and the atomic transition. This detuning ensures that the absorption probability for photons from a beam counter-propagating relative to the atomic velocity is larger than for a co-propagating beam, which results in an absorption-induced cooling force.

Due to the requirement on the light-atom detuning, laser cooling has been limited to relatively few atomic species that possess closed (or almost closed) transitions in the visible or near infrared regions of the spectrum. Nevertheless, there may exist experimentally realistic scenarios for the optical cooling of a larger class of polarizable particles with a more complicated level structure. In order to cool a target with laser light, the average frequency of the emitted light $\overline{\omega}_{em}$ must exceed the incident light frequency ω_i. To cool an arbitrary target, $\overline{\omega}_{em} > \omega_i$ must be achieved in a way that does not rely heavily on the target's internal level structure.

One way to influence directly the spectrum of the emitted light is to place the target in a "colored vacuum" [6], where the density of electromagnetic modes $\rho(\omega)$ is strongly frequency dependent. We have set up an experiment to observe cavity-induced forces from coherent scattering, as predicted for two-level atoms inside a resonator [7, 8]. However, and much to our surprise, we found that above a certain threshold incident intensity the atomic sample cooperatively emits much more light into the resonator than expected for a collection of independent atoms. At the same time, we observe emission-induced, velocity-dependent forces many times stronger than predicted for single particles, leading to temperatures well below both the atomic [1] and cavity Doppler limits [7, 8].

2 Motivation: Cavity cooling by emission into a colored vacuum

The Purcell effect [9], i.e., the alteration of spontaneous emission in a vacuum with a modified electromagnetic mode spectrum, was extensively studied at a time when the atomic center-of-mass motion was not at the center of attention [10, 11]. In 1991, Mossberg *et al.* proposed that the modified spontaneous emission inside a resonator should give rise to new velocity-dependent forces that could be used for the laser cooling of free two-level atoms [6]. Cirac, Zoller, and coworkers applied similar ideas to trapped ions [12]. The most significant contributions are due to Helmut Ritsch and coworkers, who developed quantum and semiclassical descriptions to model the behavior of single atoms and atomic ensembles moving inside a resonator pumped on-axis [7, 13]. At low saturation of atomic transitions, the cooling can be interpreted in terms of coherent (classical) scattering of radiation, which can give rise to dissipative forces whose sign is independent of the target level structure (cavity Doppler cooling) [8, 14]. Experimental evidence for resonator-induced forces has been obtained in cavity QED experiments at Caltech and in Garching [15].

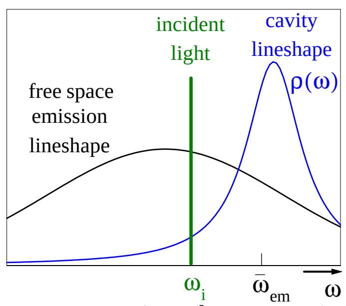

Fig. 1. Schematic representation of resonator-induced cooling.

Laser cooling requires that the average emission frequency $\overline{\omega}_{em}$ exceed the incident frequency ω_i. The probability of emission at a particular frequency ω_{em} is proportional to the electromagnetic mode density $\rho(\omega_{em})$, which varies strongly with frequency in a cavity [9, 10]. Therefore cooling of a target can be expected if a resonator with sufficiently large resonance area $\int \rho(\omega)d\omega$ is tuned to the blue of the incident light frequency ω_i (Fig. 1), thereby enhancing the high-energy part of the emission spectrum and increasing the average emission frequency above ω_i.

This shift in the emission spectrum by means of a resonator can be applied to the cooling of both internal and external degrees of freedom. In the simple case of center-of-mass cooling by (classical) coherent scattering, the frequencies of the emitted and the incident photon are related by the two-photon Doppler effect [14]. However, even in the cases of Raman scattering or collective emission, the target will lose energy in any process that satisfies $\overline{\omega}_{em} > \omega_i$.

3 Observation: Collective-emission-induced forces

Our experiments on resonator-induced forces are performed using a falling cloud of cesium atoms [16]. The sample is prepared in a magneto-optical trap (MOT) located inside a near-confocal optical resonator (Fig. 2). The resonator of length $L = 7.5$ cm has a finesse $F = 1000$, corresponding to a linewidth $\kappa/2\pi = 2$ MHz for the TEM_{00} mode with a waist size of $w_0 = 100$ μm. Mirror spherical aberration and a deviation from confocality [16] lead to a quadratic dependence of mode frequency on transverse mode number [17], which results in a multimode resonator linewidth of approximately 200 MHz. The mode density is maximized at a detuning of -200 MHz relative to the TEM_{00} resonance. At this detuning, the resonant volume extends 2.5 mm $\times$ 800 μm $\times$ 7.5 cm in the x, y, and z directions, respectively.

The incident light is provided by a distributed-Bragg reflector diode laser operating near 852 nm, whose linewidth is narrowed via optical feedback to less than 10 kHz [18], and whose frequency is actively stabilized relative to the Cs atomic transition with a long-term stability of 2 MHz. The incident light forms a linearly polarized standing wave along the x-axis that intersects the cavity axis near the cavity center. The incident beam size is $w_0 = 600$ μm, corresponding to a single-beam intensity up to $I/I_s = 2500$, where $I_s = 1.1$ mW/cm^2 is the saturation intensity. The light-cavity detuning is stabilized by means of a weak auxiliary beam coupled into the TEM_{00} mode of the cavity. For the observation of emission-induced forces, this beam is turned off with an acousto-optical modulator and a mechanical shutter, while the cavity length is held fixed at a variable offset relative to the locking point.

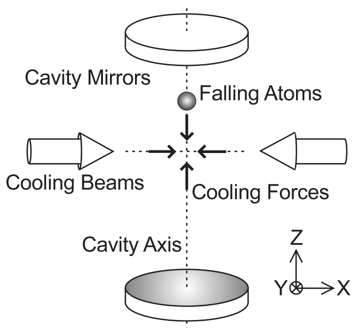

Fig. 2. Setup for observing emission-induced forces in the xz-plane.

The atomic sample is dropped from variable height (0 mm to 5 mm) above the incident light in order to prepare it at different mean initial velocities between $v_0 = 0$ and $v_0 = 30$ cm/s, where the maximum drop height is limited by thermal expansion of the cloud to a size larger than the cavity mode volume. When the atoms have fallen into the incident-beam volume, they are illuminated for a variable time between 100 μs and 25 ms. Subsequently, the distribution of arrival times in a region 2 cm below is measured with a resonant light sheet [19]. A delay (advance) of the average arrival time corresponds to a vertical deceleration (acceleration) of the sample, while a change in the width of the distribution indicates a change in the vertical rms velocity and kinetic temperature. We also observe the atomic motion in the xz-plane directly by means of fluorescence images of the falling cloud taken at various times (Fig. 4).

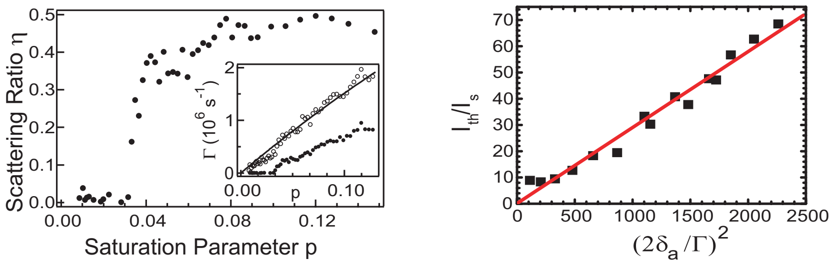

Fig. 3. (a) Fractional power emitted into a single direction of the resonator at $\delta_a/2\pi$ = -78 MHz as a function of single-beam saturation parameter p. The inset shows the scattering rate into free space Γ_{fs} (open circles) and into the cavity Γ_c (solid circles). (b) Threshold intensity I_s for collective emission as a function of light-atom detuning. $\Gamma/2\pi$ = 5.3 MHz is the atomic linewidth.

Since only photons emitted into the resonator can contribute to the resonator-induced force, an important quantity is the ratio $\eta = P_c/P_{fs}$ of the power P_c emitted into a single resonator direction relative to the power P_{fs} emitted into free space. For a resonator with degenerate modes, η is proportional to the solid angle subtended by the simultaneously resonant modes and to the finesse of the resonator [11, 14]. From the measured finesse and transmission pattern of the resonator, we calculate a value η_s = 0.05 for an atom on the resonator axis [14]. This value is consistent with the observed frequency tuning of the the cavity by the MOT cloud, and is also confirmed at low incident intensity by measuring P_c and P_{fs} using calibrated photodiodes. However, at an incident intensity above a certain threshold value I_{th}, we observe a sharp increase in η to values between 0.5 and 1 (Fig. 3a). The threshold intensity is proportional to the square of the detuning δ_a from the $6S_{1/2}, F_g = 4 \rightarrow 6P_{3/2}, F_e = 5$ transition (Fig. 3b). The light emerging from the resonator, as observed with a charged-coupled device (CCD) camera, also changes characteristically: Below threshold we observe a diffuse pattern that corresponds to the cavity multimode structure, while above threshold the light is emitted in form of bright spots appearing randomly within the resonance area.

The cooperative emission into the resonator is accompanied by strong forces on the falling atoms. If the cavity is tuned off resonance, only recoil-heating of the falling MOT cloud by free-space scattering is observed, while the mean arrival time is unchanged. If, on the other hand, the cavity is tuned on-resonance anywhere within the 200 MHz wide multimode linewidth, the velocity of the falling cloud is reduced by the collective emission, as Figs. 4c,d reveal. (Figs. 4a,b shows the falling and expanding cloud with no applied light for comparison.) The pictures a,c and b,d have been taken at t = 20 ms and t = 40 ms after the drop time, respectively, and in the cases c,d the horizontal standing wave has been applied for 4 ms at t = 15 ms.

The slowing is also evident in the time-of-flight (TOF) signal, where a second peak appears whose delay increases with light exposure time (Fig. 5a). For sufficiently long exposure times ranging between 100 μs and 5 ms depending on intensity and light-atom detuning, the fall time, i.e., the time difference between the extinction of the light and the arrival of the delayed atom sample, becomes constant, indicating that the falling cloud has been stopped (Fig. 5b) [16].

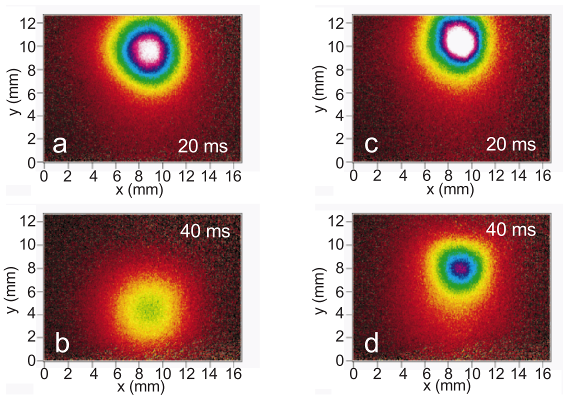

Fig. 4. Fluorescence images of the falling cloud. The pictures a,b show the falling MOT with no light applied. For the pictures c,d the horizontal standing wave has been applied at t = 15 ms for 4 ms with a near-resonant cavity, which changes the average vertical velocity of the cloud, as well as the expansion rate in the xz-plane.

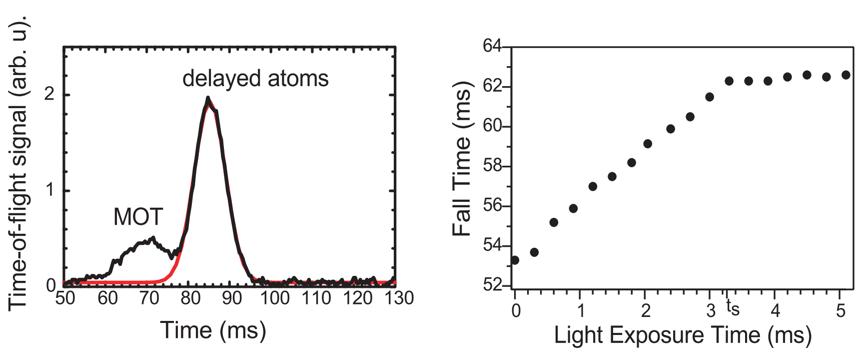

Fig. 5. (a) Time-of-flight signal of the falling cloud for $\delta_a/2\pi$ = -63 MHz and I/I_s = 16. The colored line is a Gaussian fit to the signal of the delayed fraction. (b) Fall time t_f as a function of light exposure time t_e.

As the atoms are illuminated by the horizontal standing wave, we observe not only a slowing of the cloud, but also a changing width of the delayed peak, indicative of cooling of the delayed part of the sample [16]. Within typically 0.4 ms, the temperature is reduced to values between 10 μK and 15 μK. For longer exposure times, the temperatures both along z and x remain constant in spite of substantial recoil heating by free-space scattering. The lowest temperatures are observed if the incident intensity is only slightly above threshold for collective emission. A further reduction in the kinetic temperature down to $T_z = 7\mu$K is attained if the incident light is slowly extinguished with a time constant of 400 μs. Note that since the cavity-induced force is based on momentum transfer from the incident (horizontal) to the emitted (vertical) field [14], a nonzero horizontal force is expected even for a vertically oriented resonator.

Table I summarizes the observed opto-mechanical effects at a free-space scattering rate of $\Gamma_{fs} = 3 \times 10^6 s^{-1}$, and compares them to the expected values [14] for single two-level atoms. All measured values are indicative of forces at least ten times larger than predicted by the single-atom model [7, 8].

Table I: Expected and observed emission-induced effects on atoms

quantity	expected for single atoms	observed value
scattering ratio η	0.05	0.4 to 1
maximum deceleration	$a = 90$ m/s^2	$a = 1500$ m/s^2
vertical temperature	$T_z = 190$ μK	$T_z = 7$ μK
horizontal temperature	$T_x = 780$ μK	$T_x = 11$ μK

The observed collective-emission process is consistent with Raman lasing between magnetic sublevels (Fig. 6). Optical pumping by the linearly polarized incident wave on a transition $F_g = 4 \rightarrow F_e = 5$ produces larger populations of magnetic sublevels with lower $|m|$, where m is the magnetic quantum number along the polarization axis. The inversion created between the magnetic sublevels in combination with m-dependent light shifts can give rise to Raman gain on a transition $m \rightarrow m+1$ ($m \rightarrow m-1$) for positive (negative) m. Note that a difference in light shifts for different magnetic sublevels, which arises from the different magnitudes of the Clebsch-Gordon coefficients, is necessary (Fig. 6). Without it, the gain, e.g., on the transition $m = 0 \rightarrow m = 1$, would be negated by absorption on the transition $0 \rightarrow -1$. When the differential light shift ΔU is included, the two-photon absorption is peaked at a different frequency than the two-photon gain, producing a net Raman gain in a certain frequency range.

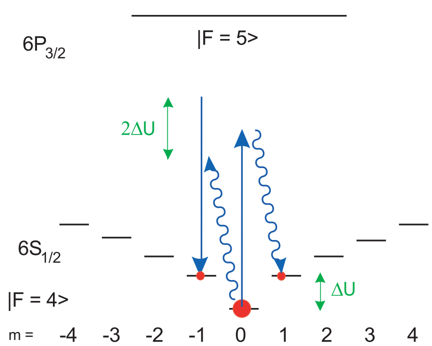

Fig. 6. Raman gain arises from the different populations of ground-state magnetic sublevels in combination with m-dependent light shifts. The straight lines represent incident photons, while the wavy lines represent cavity photons.

Several observations are consistent with Raman gain between magnetic sublevels. For a vertically polarized incident standing wave, a 400 mG magnetic field applied in the xy-plane inhibits collective emission, presumably because Larmor precession destroys the polarization, while a similar field applied along z stabilizes the collective emission. Second, for vertical incident polarization, the emitted circularly polarized light couples more strongly to the resonator than for horizontal incident polarization, leading to stronger lasing and a two times larger number of slowed atoms. Using microwave spectroscopy, we have observed a collective-emission-induced change of the magnetic sublevel populations above laser threshold that is consistent with our expectations for the Raman lasing process. Finally, the lack of lasing at red detunings $\delta_a/2\pi <$ -160 MHz is explained by depolarization of the atomic sample due to excitation to the $F_e = 4$ hyperfine excited state and decay to $F_g = 3$. We have also observed collective emission at detunings much larger than the excited state hyperfine structure, up to values of $\delta \approx -2$ GHz. However, this emission process is qualitatively different from that described above: the magnetic field sensitivity is reduced, and large cavity-to-free-space scattering ratios up to $\eta \approx 80$ are observed. The mechanical effects associated with collective emission at these large detunings will be studied further.

In the single-atom model of cavity Doppler cooling [7, 8] the symmetry between the blue and the red Doppler scattering sidebands is broken by the detuning of the cavity relative to the incident light. However, in the present case we observe cooling even in regions where the multimode cavity lineshape, as characterized by the cavity-to-free-space scattering ratio $\eta(\omega)$, is flat in frequency. Therefore some other mechanism must lead to a preference of deceleration over acceleration, and cooling over heating. Note that because of the mode competition mechanism inherent in lasing even a small initial asymmetry of the gain between the blue and the red Doppler sideband could be sufficient to make the atoms emit into the cooling sideband only.

Asymmetric emission inside a resonator with a flat mode spectrum $\eta(\omega)$ could arise from a combination of amplitude and frequency modulation similar to single-sideband modulation. An atom moving along a standing-wave resonator experiences an amplitude-modulated emission rate into the cavity, since the coupling to the resonator mode is maximum at the antinodes and vanishes at the nodes. At the same time, the position-dependent light shift in the standing wave can result in a modulation of the transition frequency. As the atom moves, both amplitude and frequency modulation occur at the Doppler frequency, with a relative phase that depends on the lights shift and therefore on the light-atom detuning. For the correct sign of the atomic polarizability, emission on the blue Doppler sideband may be stronger than on the red sideband, which in combination with optical gain might lead to strong, collective-emission-induced cooling. Such a model, if quantitatively verified, could explain the dependence on the sign of the light-atom detuning, and the role of the cavity even when the mode spectrum is flat.

The apparent generality of the present technique suggests a number of future directions. Collective Raman emission between magnetic sublevels of molecular states, and the accompanying mechanical effects, are worthy of investigation. Various extensions of the cooling technique in cesium may also be explored: The addition of a second horizontal standing wave orthogonal to the first should extend the observed cooling from two dimensions to three, and emission-induced cooling of an atomic vapor at room temperature should be possible if the total Raman scattering rate into the cavity is larger than the Doppler width of the vapor. We emphasize that previous laser cooling techniques have been single-atom methods, where the cooling performance deteriorates with increasing atom number or density. Laser cooling based on collective effects is likely to be different in both its scaling properties and its limitations.

We would like to thank C. Chin, T.W. Hänsch, M. Lukin, D. Pritchard, and H. Ritsch for stimulating discussions and suggestions. This work was supported in parts by the ARO under MURI grant Y-00-0005-02.

References

[1] T. W. Hänsch and A. L. Schawlow, Opt. Commun. **13**, 68 (1975).

[2] D.J. Wineland and H. Dehmelt, Bull. Am. Phys. Soc. 20:637 (1975).

[3] See, e.g., the contributions by Bergquist *et al.*, Blatt *et al.*, and Grangier *et al.* in this volume, and references therein.

[4] See, e.g., the contributions to the BEC Nobel Symposium in this volume.

[5] D. G. Fried, T. C. Killian, L. Willmann, D. Landhuis, S. C. Moss, D. Kleppner, and T. J. Greytak, Phys. Rev. Lett. **81**, 3811 (1998).

[6] T. W. Mossberg, M. Lewenstein, and D. J. Gauthier, Phys. Rev. Lett. **67**, 1723 (1991); M. Lewenstein and L. Roso, Phys. Rev. A **47**, 3385 (1993).

[7] P. Horak, G. Hechenblaikner, K. M. Gheri, H. Stecher, and H. Ritsch, Phys. Rev. Lett. **79**, 4974 (1997).

[8] V. Vuletić and S. Chu, Phys. Rev. Lett. **84**, 3787 (2000).

[9] E. M. Purcell, Phys. Rev. **69**, 681 (1946).

[10] D. Kleppner, Phys. Rev. Lett. **47**, 233 (1981); P. Goy, J. M. Raimond, M. Gross, and S. Haroche, *ibid.* **50**, 1903 (1983); R. G. Hulet, E. S. Hilfer, and D. Kleppner, *ibid.* **55**, 2137 (1985); W. Jhe, A. Anderson, E. A. Hinds, D. Meschede, L. Moi, and S. Haroche, *ibid.* **58**, 666 (1987), J. J. Childs, K. An, M.S. Otteson, A.R. Dasariand M. S. Feld

[11] D. J. Heinzen, J. J. Childs, J. E. Thomas, and M. S. Feld, *ibid.* **58**, 1320 (1987); D. J. Heinzen and M. S. Feld, *ibid.* **59**, 2623 (1987).

[12] J. I. Cirac, A. S. Parkins, R. Blatt, and P. Zoller, Opt. Commun. **97**, 353 (1993); J. I. Cirac, M. Lewenstein, and P. Zoller, Phys. Rev. A **51**, 1650 (1995).

[13] G. Hechenblaikner, M. Gangl, P. Horak, and H. Ritsch, Phys. Rev. A **58**, 3030 (1998); M. Gangl and H. Ritsch, *ibid.* **61**, 011402 (2000); M. Gangl and H. Ritsch, *ibid.* **61**, 043405 (2000); M. Gangl, P. Horak, and H. Ritsch, J. Mod. Opt **47**, 2741 (2000); M. Gangl and H. Ritsch, Eur. Phys. J. D **8**, 29 (2000); P. Domokos, P. Horak, and H. Ritsch, J. Phys. B **34**, 187 (2001); M. Gangl and H. Ritsch, Phys. Rev. A **64**, 063414 (2001).

[14] V. Vuletić, H. W. Chan and A. T. Black, Phys. Rev. A **64**, 033405 (2001).

[15] P. Münstermann, T. Fischer, P. Maunz, P. W. H. Pinkse, and G. Rempe, Phys. Rev. Lett. **82**, 3791 (1999); C. J. Hood, T. W. Lynn, A. C. Doherty, A. S. Parkins, and H. J. Kimble, Science **287**, 1447 (2000).

[16] H.W. Chan, A.T. Black, and V. Vuletić, quant-phys/0208100 (2002).

[17] V. F. Lazutkin, Opt. Spectrosc. **24**, 236 (1968) [Opt. Spektrosk. **24**, 453 (1968)].

[18] B. Dahmani, L. Hollberg, and R. Drullinger, Opt. Lett. **12**, 876 (1987).

[19] P. D. Lett, R. N. Watts, C. I. Westbrook, W. D. Phillips, P. L. Gould, and H. J. Metcalf, Phys. Rev. Lett. **61**, 169 (1988).